Capture and flocculation of toxic cyanobacteria by amphiphilic peptide dendrimers for mitigating harmful blooms

Heng Zheng, Pier-Luc Tremblay, Wang Chen, Qi Wang, Danni Hu, Yuanzheng Huang, Xiaoxuan Liu, Cheng-Cai Zhang, Ling Peng, Tian Zhang

Capture and flocculation of toxic cyanobacteria by amphiphilic peptide dendrimers for mitigating harmful blooms

Authors

Heng Zheng[ab#], Pier-Luc Tremblay[bcd#], Wang Chen[d], Qi Wang[c], Danni Hu[c], Yuanzheng Huang[e], Xiaoxuan Liu[e], Cheng-Cai Zhang[df], Ling Peng[g*], Tian Zhang[*abcd]

[#]These authors contributed equally to this work.

[*]**Corresponding authors**: tzhang@whut.edu.cn (T.Z.), ling.peng@univ-amu.fr (L.P.)

Affiliations

[a]School of Resources and Environmental Engineering, Wuhan University of Technology, Wuhan 430070, PR China

[b]Sanya Science and Education Innovation Park, Wuhan University of Technology, Sanya 572024, PR China

[c]School of Chemistry, Chemical Engineering, and Life Science, Wuhan University of Technology, Wuhan 430070, PR China

[d]Institut WUT-AMU, Wuhan University of Technology, Wuhan 430070, PR China

[e]State Key Laboratory of Natural Medicines and Jiangsu Key Laboratory of Drug Discovery for Metabolic Diseases, Center of Advanced Pharmaceuticals and Biomaterials, China Pharmaceutical University, Nanjing, 210009, PR China

[f]State Key Laboratory of Freshwater Ecology and Biotechnology, Institute of Hydrobiology, Chinese Academy of Sciences, Wuhan, 430072, PR China

[g]Aix Marseille University, CNRS, Center Interdisciplinaire de Nanoscience de Marseille, UMR 7325, Marseille, 13288, France

Abstract

Harmful and toxic cyanobacterial blooms in freshwater constitute critical environmental problems and are becoming more frequent as a consequence of global climate change. One mitigation strategy is flocculation, which could be achieved with treatment by highly efficient, non-toxic, and biodegradable agents. Here, we report two amphiphilic peptide dendrimers (AmPDs), KK_2 and KK_2K_4, for the removal of the toxic and bloom-forming cyanobacterium *Microcystis aeruginosa* from freshwater. KK_2 and KK_2K_4 are composed of a hydrophobic alkyl chain and a positively charged polylysine dendron of the first and second generation, respectively. Owing to electrostatic interactions with the negatively charged cell surface of *M. aeruginosa*, KK_2 and KK_2K_4 could quickly capture the cyanobacterial cell population via flocculation at very low concentrations. When combined with the natural clay sepiolite, the two AmPDs were even more efficient in promoting cell flocculation. The most performant system, with 3.0 mg/L KK_2K_4 and sepiolite clay, could remove 97.1% of *M. aeruginosa* within 15 min by forming stable flocs. Remarkably, such a system was able to trap toxin molecules released by cyanobacterial cells, thus limiting its destructive impact on ecosystems. This study demonstrates how self-assembling dendrimer materials can resolve cyanobacterial blooms, providing an innovative solution to this environmental challenge.

Keywords

Cyanobacterial bloom, Toxin, Amphiphilic dendrimer, Flocculation, Sepiolite clay, Negatively charged microbial surface

1. Introduction

Harmful algal blooms are a serious environmental, water quality, and public health issue worldwide. Specifically, cyanobacterial bloom refers to the excessive growth of photoautotrophic cyanobacteria, which form dense biomass and produce toxins, contaminating water and causing adverse effects on human health or even death of domestic and livestock animals [1,2]. In recent years, the frequency, timespan, and intensity of cyanobacterial blooms have increased because of anthropogenic activities [3-5]. This environmental situation is now a major concern for the usage, sustainability, and safety of freshwater reserves with an important economic impact estimated to cost tens of billions of US dollars every year [6]. Industrial, agricultural, and domestic wastewater discharges have led to water body eutrophication, which generates excellent nutritional conditions for cyanobacterial proliferation [1,7]. In addition, many cyanobacteria species prefer warmer temperatures and are benefitting from climate changes, which likely increases the occurrence of harmful blooms [8].

In particular, cyanobacterial blooms are associated with the production of a large amount of toxins, posing a serious threat to public health. For example, one of the most commonly observed harmful cyanobacteria, *Microcystis aeruginosa*, generates multiple microcystin congeners (MCs) that are hepatic toxins and potentially carcinogenic for humans and other living organisms [9,10]. Among the MCs, the microcystin-LR (MC-LR) is the most abundant and toxic [11]. MC-LR and other MCs are cyclic peptides made by non-ribosomal peptide synthetases, which are relatively stable, and thus difficult to remove from waterbodies affected by cyanobacterial proliferation. In view of the

negative impact of cyanobacterial blooms on ecosystems, human health, and the economy, many studies have been undertaken to develop efficient and eco-friendly mitigation strategies.

Methods to remediate cyanobacterial contaminations include physical, chemical, and biological approaches. Physical strategies such as ultrasonic cracking and air flotation devices are often costly, only applicable to small scale, and can increase the transient release of cyanotoxins [12,13]. Chemical approaches mainly employed oxidants, e.g. copper sulfate, hydrogen peroxide, or diverse herbicides or photocatalysts [14,15]. Large amounts are required to solve algal blooms, augmenting the risk that these molecules, which are also toxic for non-target species, accumulate in the environment. In addition, such treatments often lead to cyanobacterial cell lysis, and thus increase the release of cyanotoxins [16]. Lastly, biological methods exploit predator-prey relationships, nutritional competition between cyanobacteria and harmless organisms, parasitism, or virus infection [17,18]. However, these strategies are often considered too slow for the treatment of sudden cyanobacterial blooms [17,19]. Therefore, an alternative methodology still needs to be developed for the efficient eradication of toxic cyanobacteria.

One of the most cost-effective and convenient technologies for the removal of harmful cyanobacteria from lakes and/or raw water supply is flocculation [20,21]. The floc-and-sink method aims at displacing cyanobacteria from the water column to the sediment, thus limiting their negative impact [22,23]. However, conventional inorganic flocculants

such as metal salts and polyaluminium chloride are generally not suitable for large-scale floc-and-sink removal of harmful algal blooms due to their toxicity for non-target species [20]. Organic flocculants, including chitosan, tannin, and cationic starch, have also different shortcomings such as low efficiency and high cost [24,25]. Among extensively studied flocculants, natural clays such as sepiolite are some of the few that have been applied in situ for the treatment of algal blooms [26]. Clays are abundant and usually non-toxic, and their flocculation process prevents the release of toxins [27]. Still, their overall efficiency is low, and their surface usually needs modifications with other compounds to increase the electrostatic attraction of negatively charged cyanobacteria [28,29].

Amphiphilic peptide dendrimers (AmPDs) developed in recent years are tunable organic complex molecules made of hydrophobic alkyl chains and hydrophilic peptides [30]. Until now, non-toxic, biocompatible, and biodegradable AmPDs have mainly been designed and explored for biomedical purposes [31]. For instance, they are employed for bioimaging, drug delivery, as transfection vectors, or agents against pathogenic microbes [32-35]. Outside of the biomedical field, applied research on AmPDs has not yet been reported. We report here the use of AmPDs bearing a strong positively charged surface for the removal of negatively charged microbes such as cyanobacteria for mitigating cyanobacterial contaminations. Specifically in this study, two AmPDs, KK_2 and KK_2K_4 (Scheme 1), were evaluated for the flocculation and sinking of the toxic cyanobacterium *M. aeruginosa*. KK_2 and KK_2K_4 are composed of a hydrophobic alkyl chain and a positively charged poly(L-lysine) dendron of the first and second generation,

respectively. We assessed the cyanobacterial flocculation activity of KK_2 and KK_2K_4 alone or in combination with sepiolite clay under different environmental conditions. We also examined the mechanisms involved in the capture by KK_2 and KK_2K_4 of *M. aeruginosa* cells. Our results showed that the AmPDs were highly efficient for the flocculation and removal of *M. aeruginosa* populations. In addition, AmPDs removed nitrogen nutrients central to the proliferation of cyanobacteria in freshwater. More importantly, the AmPDs, when combined with sepiolite, became even more active and rapidly captured toxic cyanobacteria without breaking them, thus avoiding a transient increase of MCs in water.

2. Experimental section

2.1. Cultivation of *M. aeruginosa*

The model cyanobacterial strain *M. aeruginosa* PCC 7806 was obtained from the Institute of Hydrobiology of the Chinese Academy of Sciences (Wuhan, China). Axenic *M. aeruginosa* was grown at 30 °C with agitation at 150 rpm in BG-11 medium [36]. The microbial cultures were maintained under light at an intensity of 45 μmol photons/m^2/s with a 12-h light/dark cycle. For flocculation experiments with the AmPDs and sepiolite, *M. aeruginosa* was first cultivated until reaching the exponential phase. *M. aeruginosa* cell growth and density were monitored by both counting cells with a hemacytometer and an Eclipse Ti2 inverted microscope (Nikon, Tokyo, Japan) and measuring the optical density (OD) at 680 nm with a UV-Vis Evolution 220 spectrophotometer (Thermo Fisher Scientific, Waltham, MA, USA).

148

149 **2.2. Synthesis of KK_2 and KK_2K_4 nanoassemblies**

150 For the synthesis of AmPDs, the hydrophilic and hydrophobic segments were prepared
151 separately and then conjugated via click chemistry as previously described [37]. Briefly,
152 the hydrophobic portion consists of a double-tailed alkyl chain with azide groups, while
153 the hydrophilic part constitutes the dendritic peptide segment. The synthesis of the latter
154 began with propargylamine as the starting material and utilized Boc-protected lysine by
155 alternating coupling and deprotection steps. The two segments were joined together
156 through a copper-catalyzed click reaction between the alkyne and azide groups. Copper
157 ions were chelated and subsequently removed with ammonium chloride followed by
158 deprotection to obtain the target products. After washing and further purification by
159 dialysis, the AmPDs were lyophilized. During the synthesis process, the structure of both
160 KK_2 and KK_2K_4 and their intermediates were validated by ^1H nuclear magnetic resonance
161 spectroscopy as previously described [38]. The main difference between KK_2 and KK_2K_4
162 is that the former bears a simpler and smaller peptide dendron exhibiting four terminal
163 amino groups, while the latter is a more complex and larger molecule with eight terminal
164 amino groups.

165

166 In our previous studies [37,38], both AmPDs were shown to readily form, in aqueous
167 environments, nanoassemblies with a positively charged surface (Scheme 1). To achieve
168 that here, lyophilized KK_2 and KK_2K_4 were suspended in a 10 mM sodium phosphate
169 buffer (pH 7.4) at a concentration of 50 mg/L followed by storage for at least 12 h at
170 4 °C. Transmission electron micrographs (TEM) of the AmPD nanoassemblies were

taken with a JEM-2100Plus system (JEOL, Tokyo, Japan) at an accelerating voltage of 200 kV. To start flocculation experiments, different volumes of these stock solutions were mixed with *M. aeruginosa* cultures.

2.3. Flocculation experiments

M. aeruginosa flocculation experiments were conducted with concentrations of KK_2 or KK_2K_4 ranging from 0.0 to 7.0 mg/L. Where indicated, 50.0 to 325.0 mg/L of sepiolite (Lingshou County Wancheng Mineral, Shijiazhuang, China) was also added. Sepiolite particles were washed at least 3 times with deionized water before usage.

Standard flocculation tests were done in triplicate with 10-mL *M. aeruginosa* cultures at a density of ca. 3.0×10^6 cells/mL, a temperature of 30 °C, and under visible light at an intensity of 45 μmol photons/m^2/s. The cell density for this experiment was selected because it is representative of cyanobacterial blooms in lake water [39]. Glass tubes employed for the flocculation tests had a diameter of 16 mm and a height of 50 mm. Where indicated, the salinity of the cell culture was adjusted with 1.0 M NaCl while the pH was adjusted with 0.1 M HCl or NaOH. Agitation was done at different speeds with a MS-M-S10 magnetic stirrer (DLAB, Beijing, China). AmPDs with or without sepiolite were first mixed with the cell culture at 600 rpm for 1 min. Where indicated, the initial agitation speed was slower at 150 or 300 rpm, which had no significant impact on the flocculating performance of KK_2 and KK_2K_4 (Fig. S1). Next, the suspension was maintained at 150 rpm for 14 min. The agitation was then completely stopped and the culture was left on a stand. The beginning of this step was considered as the time 0 of the

194 flocculation process. Subsequently, 1-mL samples were taken 2 cm below the surface of
195 the cell culture at different time points and the $OD_{680\ nm}$ was measured with a UV-Vis
196 Evolution 220 spectrophotometer (Thermo Fisher Scientific). In addition, the turbidity of
197 samples was quantified in Formazin Turbidity Unit (FTU) by comparing it
198 spectrophotochemically with formazin standards as previously described [40]. Total
199 nitrogen and phosphorus were measured in the samples with the Chinese national
200 standard method GB/T 11894-1989 and GB/T 11893-1989. Lastly, to assess the flocs'
201 stability, the cell cultures were filtered after the different flocculation treatments with a 60
202 μm nylon membrane. The $OD_{680\ nm}$ of the filtrates was then measured. Here, it is
203 expected that flocs with sufficient cohesiveness and size will be retained by the filter
204 while flocs that are not cohesive will be broken by the physical barrier of the filter and
205 pass in the filtrates.
206
207 **2.4. Characterization of the flocs and microcystin-LR quantification**
208 Bright-field light micrographs of the flocs and other samples were taken at a
209 magnification of 100× with an Eclipse Ti2 inverted microscope (Nikon) as described
210 previously [41]. Scanning electron microscopy (SEM) analyses of *M. aeruginosa* flocs
211 were completed with a MIRA system (TESCAN, Brno, Czech Republic) at an
212 accelerating voltage of 15 kV and a sample preparation method reported earlier [42].
213 Briefly, the cyanobacteria flocs were fixed overnight at 4 °C with 2.5% glutaraldehyde.
214 After that, the samples were washed three times with a 10 mM sodium phosphate buffer
215 (pH 7.4). Next, the cells were dehydrated with an ethanol gradient of 30%, 50%, 70%,

85%, and 90%. In the final preparation step, samples were freeze-dried for 12 h before being sputter-coated with gold for SEM observation.

The zeta potentials of the different flocculants and *M. aeruginosa* flocs were measured with a Zetasizer Nano ZS analyzer (Malvern, Malvern, United Kingdom). The concentration of extracellular MC-LR molecules released by *M. aeruginosa* in the growth medium was measured with an ELISA kit (Institute of Hydrobiology of the Chinese Academy of Sciences) as previously described [43] and a Multiskan FC multi-plate reader (Thermo Fisher Scientific).

2.5. Cyanobacterial cell viability

The viability of *M. aeruginosa* was evaluated by detecting the red autofluorescence of chlorophyll (Chl) molecules as previously described [44,45]. The Chl content of metabolically active cyanobacteria usually remains constant. Conversely, the death or senescence of cyanobacteria is associated with a massive degradation of Chl molecules [46]. Thus, cyanobacterial cells emitting a red fluorescence during this assay are considered to be metabolically active and viable. Here, an untreated cyanobacterial population as well as flocculation reactions at different time points were first vortexed for 30 s. 5 μL of these preparations were deposited on microscope slides followed by observation with an Eclipse Ti2 inverted microscope (Nikon) at a 540-580 nm excitation wavelength, a 595 nm dichroic beam splitter, and a 600-660 nm emission wavelength [46]. *M. aeruginosa* viability (V) after the different treatments was calculated with Eq. 1:

239 $V\ (\%) = n_{Vf} / n_{Vi} \times 100$ Eq. 1

240 where n_{Vi} is the initial number of cells emitting red fluorescence before the flocculation
241 treatment and n_{Vf} is the final number of fluorescent cells after flocculation.

242

243 **2.6. Statistical analysis**

244 Data are reported as means ± standard deviation (n ≥ 3). The Student's t-test was
245 employed to determine statistical significance between groups. * indicates p-values ≤
246 0.01.

247

248 **3. Results and discussion**

249 **3.1. Effective capture of *M. aeruginosa* by dendrimers via electrostatic interactions**

250 Because of their positively charged surface, we expect that nanoassemblies of the AmPD
251 KK_2 and KK_2K_4 will form strong electrostatic interactions with negatively charged *M.*
252 *aeruginosa* (Scheme 1) [47]. This, in turn, should lead to cell aggregation and floc
253 formation. To evaluate this hypothesis, a *M. aeruginosa* population was exposed to
254 different concentrations of either KK_2 or KK_2K_4 nanoassemblies exhibiting a diameter of
255 ca. 67-170 nm (Fig. S2). After 30 min at room temperature and circumneutral pH, KK_2
256 at an optimal concentration of 6.0 mg/L removed 96.3 ± 2.2% of cyanobacterial cells by
257 flocculation (Fig. 1ab). Under the same conditions, a lower KK_2K_4 concentration of 5.0
258 mg/L removed 97.7 ± 1.2% of cyanobacterial cells. The higher efficiency of KK_2K_4
259 nanoassemblies is likely related to its larger number of branches and surficial amino
260 groups, which increases the electrostatic attraction strength with *M. aeruginosa* cells.
261 Higher concentrations of 7.0 mg/L for KK_2 and 6.0 or 7.0 mg/L for KK_2K_4 resulted in a

small decline of flocculation efficiencies compared to when the optimal concentration of either flocculant was added. It is possible that excessive AmPDs compromised the structural cohesiveness of the flocs, leading to a partial release of cyanobacterial cells.

Time-course studies with either KK_2 or KK_2K_4 showed that the removal process of *M. aeruginosa* cells was rapid and mostly happened within 5 min of exposure with 83.2 ± 1.4% and 90.6 ± 1.6% of flocculated cells, respectively, before reaching optimal values after 30 min (Fig. 1c). In addition, a visual inspection indicated that the dense flocs formed via cell aggregation using either KK_2 or KK_2K_4 sunk to the bottom of the test tubes (Fig. 1d). As reported in Table S1, when compared with other single inorganic and organic materials developed for the flocculation and sinking of freshwater cyanobacteria, both KK_2 and KK_2K_4 were often more efficient and faster at completing the removal of *M. aeruginosa* from the water column while requiring a lesser amount of reagent. Besides better performance, KK_2 and KK_2K_4 flocculants exhibit additional advantages. Their structures can be customized precisely for the predictable tuning of their properties such as the strength of their interactions with microbes [35,48,49], offering advantages over other materials evaluated for toxic cyanobacteria flocculation which are often ill-defined, complex, or unmodifiable. Thus, AmPDs have a large untapped potential for the future improvement of their capacity to treat cyanobacterial blooms. Furthermore, KK_2 and KK_2K_4 are also biodegradable with good biocompatibility for eukaryotic cells [50,51]. This indicates that these flocculants are unlikely to accumulate in the environment and exhibit adverse effects on the flora and fauna.

285 Next, light micrographs of *M. aeruginosa* exposed to KK_2 or KK_2K_4 were taken to
286 visualize the formation of aggregates (Fig. 2). Untreated *M. aeruginosa* mostly appeared
287 as individual cells with their characteristic morphology and green color (Fig. 2a) [52].
288 The addition of 2.0 mg/L KK_2 already caused a change in the cell aggregation with the
289 formation of grapes comprising 2-3 microbes (Fig. 2b). When the optimal KK_2
290 concentration of 6.0 mg/L was added, aggregates became more massive and included ca.
291 30 to 120 cells (Fig. 2d). A similar phenomenon was observed with KK_2K_4 where lower
292 concentrations (1.0-3.0 mg/L) of the AmPD resulted in *M. aeruginosa* aggregates of 2 to
293 8 cells (Fig. 2ef). Cyanobacterial cells exposed to the optimal KK_2K_4 concentration of 5.0
294 mg/L assembled in groups of mostly 90-120 cells (Fig. 2g).
295
296 SEM micrographs confirmed the aggregation process. Untreated cells were mainly
297 individual spheres with shape irregularities distinctive of *M. aeruginosa* (Fig. 2h). In
298 comparison, cells exposed to an optimal concentration of KK_2 formed imbricated clusters
299 (Fig. 2i). Similarly, *M. aeruginosa* clumped with KK_2K_4 into flocs made of multiple cells
300 (Fig. 2j). The main reason behind this efficient flocculation process can be ascribed to the
301 positively charged KK_2 and KK_2K_4 nanoassemblies attracting the negatively charged
302 cyanobacterial cells into a cohesive multicellular structure. While the zeta potential of a
303 high-density *M. aeruginosa* preparation was -22.6 ± 0.4 mV, KK_2 and KK_2K_4 exhibited
304 surface charges of 23.9 ± 0.3 mV and 29.1 ± 0.2 mV, respectively (Fig. 2k). Exposing the
305 cyanobacterial cells to KK_2 and KK_2K_4 resulted in flocs with weaker positive surface
306 charges of 2.8 ± 0.3 mV and 4.0 ± 0.2 mV, respectively. These results indicate that
307 AmPDs and *M. aeruginosa* nearly neutralized their respective surface charges by forming

strong electrostatic interactions, leading to cell aggregation. They also explain why KK_2K_4 with its higher positive zeta potential is more efficient than KK_2 at removing the toxic cyanobacteria from an aqueous solution.

3.2. Synergistic flocculation by dendrimers combined with sepiolite

Widely available clays such as sepiolite are often employed in situ for the flocculation of cyanobacterial bloom because of their abundance as well as low ecotoxicity (Table S2) [53-55]. However, natural clays have a low flocculating efficiency, which means that massive dosages are required, increasing expenses and possible undesired environmental impacts. Here, we assessed both KK_2 and KK_2K_4 in combination with sepiolite for the flocculation of *M. aeruginosa* (Fig. 3). In the first series of experiments, different concentrations of KK_2 and KK_2K_4 were coupled with 200.0 mg/L sepiolite, respectively (Fig. 3a). When compared to AmPDs alone, the addition of sepiolite had two beneficial effects. First, lower concentrations of AmPDs were required to remove most *M. aeruginosa* cells. 4.0 mg/L KK_2 and 3.0 mg/L KK_2K_4 with sepiolite were sufficient to flocculate and sink 96.5 ± 2.4% and 97.1 ± 2.2% of the cyanobacterial cells, respectively. Second, the removal process was twice faster and reached equilibrium after only 15 min (Fig. 3b). In fact, 88.9 ± 1.2% and 89.9 ± 2.0% *of M. aeruginosa* cells have already been removed after 5 min by KK_2 and KK_2K_4 with sepiolite, respectively. Subsequently, optimal KK_2 and KK_2K_4 concentrations were mixed with different quantities of sepiolite (Fig. 3c, Fig. S3). The sepiolite-only control (up to 325.0 mg/L) removed a negligible fraction (below 10%) of the cyanobacterial cells, illustrating the inefficiency of unmodified natural clays in the timeframe investigated. The highest flocculation

performance for both AmPDs was observed with sepiolite concentrations of 200.0-250.0 mg/L.

Light micrographs showed the flocculation of *M. aeruginosa* cells by KK_2 or KK_2K_4 with sepiolite (Fig. 4). When compared to 4.0 mg/L KK_2 alone (Fig. 4a), the addition of low concentrations of sepiolite (50.0-100.0 mg/L) already increased the size of the aggregates (Fig. 4bc). On these micrographs, sepiolite appeared as spindle-like black mineral structures. In the presence of 200.0 mg/L sepiolite and KK_2, *M. aeruginosa* aggregates became massive with hundreds of cells (Fig. 4d). A similar effect was observed when 3.0 mg/L KK_2K_4 was combined with the same concentration of sepiolite, resulting in the formation of expanded flocs (Fig. 4h).

The SEM analysis confirmed that *M. aeruginosa* cells aggregated with sepiolite spindles in complex cohesive networks maintained by the AmPDs (Fig. 4i-k). Measurements of the zeta potentials of sepiolite, sepiolite in the presence of KK_2 or KK_2K_4, and sepiolite in the presence of *M. aeruginosa* cells with KK_2 or KK_2K_4 demonstrated the importance of electrostatic interactions for the floc formation (Fig. 4l). While sepiolite alone exhibited a zeta potential of -23.2 ± 6.0 mV, the addition of KK_2 or KK_2K_4 resulted in modified clay with a positive charge of 21.6 ± 0.2 mV and 26.2 ± 0.6 mV, respectively. These results indicate that the AmPD nanoassemblies coated sepiolite particles, changing entirely their surface charge. In the presence of *M. aeruginosa* cells, the positively charged surface of modified sepiolite was neutralized and the flocs had a slightly negative charge, confirming that the cyanobacterial cells closely interacted with the AmPD coat of

sepiolite. Several reasons may explain why sepiolite improved the performance of the AmPDs for the capture and removal of *M. aeruginosa* cells from water. Sepiolite with its spindle shape has a significant specific surface area shown to range from 77 to 399 m^2/g in the literature [56], and when coated with AmPD molecules, it will form bigger flocs with a greater number of *M. aeruginosa* cells that will settle faster to the bottom. Another possible factor to consider is that multiple coated sepiolite particles may form a matrix encasing toxic cyanobacterial cells and sinking them to the bottom.

The flocculation systems combining KK_2 or KK_2K_4 and sepiolite described in this proof-of-concept study exhibited excellent performance compared to many other clay-based materials (Table S2), but may still present a challenge for practical applications since a relatively important concentration of sepiolite was required. This could lead to unwanted sediment accumulation altering local ecosystems. Consequently, we aim in future research to develop AmPD flocculating systems requiring less clay while maintaining similar efficiency. This could be achieved, for instance, by coupling KK_2 and KK_2K_4 with clay particles exhibiting different sizes, morphologies, and porosities. These factors, especially a suitable clay particle size, have a major impact on the collision efficiency with microbial cells, and thus on the flocculation process [57].

3.3. Dendrimer/sepiolite combination stabilized flocculation and obviated cell death and microcystin release

Next, the impact of KK_2 and KK_2K_4 on the viability of *M. aeruginosa* cells was evaluated by monitoring the intrinsic red fluorescence emitted by Chl molecules of intact

377 photosystems from active cells [41]. Among all the tested flocculation systems, KK_2, at a
378 concentration of 6.0 mg/L, did not impact much cell viability nor stimulate the release of
379 MC-LR, the most abundant and potent toxin generated by *M. aeruginosa* (Fig. 5ab) [1].
380 Conversely, KK_2K_4 at 5.0 mg/L considerably compromised the viability of *M.*
381 *aeruginosa* after 24 h (Fig. 5a, Fig. S4). At this time point, KK_2K_4 had killed 74.4 ± 2.0%
382 of cyanobacterial cells from the initial cell suspension. A clear inconvenience of the
383 killing effect of KK_2K_4 was that it increased 1.7 times the extracellular concentration of
384 MC-LR compared to an untreated control (Fig. 5b) [58]. This is probably because
385 damaged cyanobacteria released the cyanotoxin upon the disruption of their cell
386 membranes. It should be mentioned that dendrimers with amino terminals and an overall
387 structure similar to KK_2K_4 were recently reported to have strong antibacterial properties
388 against both Gram-positive and Gram-negative pathogenic bacteria [35,48]. These
389 molecules electrostatically interacted and accumulated around the bacterial cell wall
390 followed by membrane disruption and bacterial killing. At the concentration examined in
391 our study, this is possibly what happened with KK_2K_4.
392
393 Surprisingly, the flocculation system combining 3.0 mg/L KK_2K_4 nanoassemblies and
394 sepiolite behaved differently (Fig. 5ab). It did not induce the death of *M. aeruginosa* cells
395 or the release of MC-LR, which is completely different from the treatment with KK_2K_4
396 alone. This divergence could be due to the lower concentration of KK_2K_4 used in the
397 combination treatment, hence being less potent. It could also be related to strong
398 electrostatic interactions between sepiolite and KK_2K_4, restraining AmPD molecules from
399 penetrating the cell wall and disorganizing lipid bilayers. In addition, with KK_2K_4 and

sepiolite in combination, cyanobacterial cells remained settled to the bottom of the water column with only a small increase in viability after 72 h (Fig. S5-S7). This indicates that KK_2K_4 and sepiolite could maintain good control of the cyanobacterial population at least for several days, and not just for a short period.

More remarkably, the KK_2K_4 with sepiolite system reduced 1.5 times the concentration of MC-LR in the water compared to an untreated control. MC-LR cyclic molecules have two ionizable carboxyl groups not forming peptide bonds and thus are almost exclusively negatively charged at pH higher than 7.0 [59]. Thus, the KK_2K_4 and sepiolite flocculation system, which exhibits a strong positive charge on its surface and does not compromise the integrity of cyanobacterial cells, could also be suitable for the partial elimination of cyanotoxins exhibiting an overall negative charge. Besides MC-LR, *M. aeruginosa* releases other MC congeners that are less toxic and abundant [60]. Further work is required to determine the impact of KK_2 and KK_2K_4 with or without sepiolite on the faith of these uncommon MC congeners.

It is also of note that KK_2K_4 with sepiolite generated highly stable flocs that were not prone to quick disassembling and the unwanted release of biomass (Fig. 5c). To investigate the floc cohesiveness, *M. aeruginosa* cell suspensions before and after treatment were filtered with a nylon membrane filter. KK_2K_4 with sepiolite was the most performant system with the removal of 96.3% of microbial particles from the aqueous solution by filtration. *M. aeruginosa* flocs formed with KK_2 or KK_2K_4 were slightly less recoverable. The flocculation assay showed that both AmPDs captured and sedimented at

least 95% of the cyanobacterial cell population (Fig. 1). Upon filtration, 74.6% and 83.7% of the flocculated biomass could be recovered when KK_2 or KK_2K_4 were employed, respectively. This observation denotes that most flocs assembled via KK_2 or KK_2K_4 can be separated from the aqueous solution with only a minority fraction either too small to be filtered out or getting dismantled. KK_2 nanoassemblies with sepiolite was the worst flocculation strategy for subsequent recovery by filtration with the majority of flocculated/sedimented biomass remaining in the aqueous solution.

3.4. Removal of total nitrogen by the dendrimers

Cyanobacterial contaminations are directly caused by excessive nitrogen and phosphorus inputs from human activities [1]. While removing cyanobacteria cells, some flocculants can simultaneously adsorb nitrogen and/or phosphorus compounds [23,61]. Our results indicated that KK_2 and KK_2K_4 with or without sepiolite removed large fractions of total nitrogen, but had less impact on phosphorus (Fig. S8). For nitrogen, KK_2 was the most efficient system after a 30-minute reaction with 92.9 ± 1.9% removed from the aqueous solution. In the case of phosphorus, only KK_2 with sepiolite adsorbed a small fraction of 12.5 ± 1.8%. KK_2 and KK_2K_4 are charged positively, and thus it is not surprising that they adsorbed nitrate anions found in the cyanobacterial suspension. In this study, the cyanobacterial suspensions contained ca. 11 times more nitrate than phosphate ions. Abundant nitrate and cyanobacterial cells may outcompete phosphate for the adsorption sites on the surface of the AmPD molecules, possibly explaining why total phosphorus remained unchanged in most cases. These observations demonstrate that all the AmPD-based systems evaluated can clean concomitantly the biological agent responsible for

446 cyanobacterial contamination as well as key nitrogen pollutants responsible for this
447 harmful phenomenon.
448
449 **3.5. Cyanobacterial flocculation was dependent on salinity and pH**
450 The effect of different environmental conditions such as salinity and pH on the AmPD-
451 driven flocculation process was then investigated (Fig. 6). The salinity of the aqueous
452 solution contaminated with *M. aeruginosa* had an important impact on the efficiency of
453 the aggregation for both KK_2 and KK_2K_4 with or without sepiolite (Fig. 6ab). For
454 instance, *M. aeruginosa* removal was reduced to only 48.3 ± 2.9% and 31.3 ± 1.4% with
455 KK_2 and KK_2K_4, respectively, when the NaCl concentration was 0.17 M compared to
456 media with null ionic strength (Fig. 6a). This is likely because ions from the salt interact
457 with the surfaces of AmPDs as well as cyanobacterial cells, changing their electrical
458 charges and interfering with the formation of electrostatic interactions. An increase in
459 salinity is also known to affect the behavior of dendrimeric nanosystems in solution and
460 modify their capacity to form nanoassemblies [62]. This could be another reason why a
461 high salt concentration impeded flocculation. The addition of sepiolite did not mitigate
462 most of the negative effects of augmented salinity. KK_2 and KK_2K_4 nanoassemblies with
463 sepiolite removed only 41.1 ± 0.7% and 51.5 ± 1.3% of *M. aeruginosa* cells, respectively,
464 at the highest ionic strength evaluated (Fig. 6b). These observations indicate that the
465 AmPDs studied here are more suitable for treating freshwater contamination such as the
466 ones involving *M. aeruginosa* and may not be as efficient for cyanobacterial proliferation
467 in saltier water.
468

469 The importance of the pH for the activity of both KK_2 and KK_2K_4 combined with or
470 without sepiolite was also investigated (Fig. 6cd). The proliferation of *M. aeruginosa* is
471 favored when the pH becomes basic [63]. In addition, during algal blooms, the
472 photosynthetic activity of cyanobacteria and other microalgae increases the pH between
473 8.0 to 9.5 [64,65]. Thus, the activity of both AmPDs was evaluated at pH values from 6.0
474 to 11.0 (Fig. 6c). Even up to a pH of 10.0, both KK_2 and KK_2K_4 maintained a
475 cyanobacterial removal activity above 85.0%. At pH 11.0, the capture capacity of *M.*
476 *aeruginosa* cells by both KK_2 and KK_2K_4 collapsed. A similar pattern was observed with
477 AmPD-driven flocculation systems comprising sepiolite with cyanobacterial cell removal
478 remaining high until the pH was increased to 11.0 (Fig. 6d). In this condition, amino
479 groups at the surface of AmPDs likely lost their positive charge, which wiped out their
480 capacity to form electrostatic interactions with microbes. Nevertheless, at mild basic pHs
481 observed during cyanobacterial blooms, KK_2 and KK_2K_4 exhibited strong activities for
482 flocculation induction.
483
484 **4. Conclusions**
485 In this proof-of-concept study, we demonstrated that AmPDs harboring positively
486 charged terminals can serve for environment engineering applications to mitigate water
487 bloom via flocculation and sinking of toxic cyanobacteria. Specifically, low
488 concentrations of KK_2 and KK_2K_4 complemented with or without sepiolite removed more
489 than 95% of *M. aeruginosa* cells within 15 to 30 min. The best flocculating system
490 identified was the combination of KK_2K_4 and sepiolite clay, which quickly removed
491 97.1% of cyanobacterial cells and a significant fraction of MC-LR molecules from
492 freshwater by forming highly stable flocs. The AmPDs, which exhibit a strong surficial

positive charge, mainly captured the negatively charged cyanobacterial cells through electrostatic interactions. The AmPD molecules were also able to concomitantly remove nitrogen nutrients central to the occurrence of cyanobacterial contaminations. Based on their excellent performance, AmPDs could become a promising new category of materials for two different applications related to cyanobacterial contaminations: in-lake bloom mitigation and water treatment for human utilization. Both purposes have different requirements and additional work is necessary before concluding that AmPDs can be effectively implemented in the real world. This includes subsequent investigations that will establish the long-term effectiveness and the technical, ecological, and economic feasibility of employing AmPD flocculating systems in complex freshwater environments populated by different problematic cyanobacterial species with unique physiologies. We are actively pursuing this research direction.

Declaration of competing interest

The authors declare that they have no known competing financial interests or personal relationships that could have appeared to influence the work reported in this paper.

Data availability

Data will be made available on request.

Acknowledgements

This project was funded by the Hainan Yazhou Bay Science and Technology Bureau (No SKJC-2020-01-004) and the National Natural Science Foundation of China (No 42272355).

Appendix A. Supplementary data

References

[1] J. Huisman, G.A. Codd, H.W. Paerl, B.W. Ibelings, J.M.H. Verspagen, P.M. Visser, Cyanobacterial blooms, Nat. Rev. Microbiol. 16 (2018) 471–483. https://doi.org/10.1038/s41579-018-0040-1.

[2] Y. Zhang, J.K. Whalen, C. Cai, K. Shan, H. Zhou, Harmful cyanobacteria-diatom/dinoflagellate blooms and their cyanotoxins in freshwaters: A nonnegligible chronic health and ecological hazard, Water Res. 233 (2023) 119807. https://doi.org/10.1016/j.watres.2023.119807.

[3] H.W. Paerl, Controlling cyanobacterial harmful blooms in freshwater ecosystems, Microb. Biotechnol. 10 (2017) 1106–1110. https://doi.org/10.1111/1751-7915.12725.

[4] H.W. Paerl, T.G. Otten, Harmful Cyanobacterial Blooms: Causes, Consequences, and Controls, Microb Ecol 65 (2013) 995–1010. https://doi.org/10.1007/s00248-012-0159-y.

[5] A. Volk, J. Lee, Cyanobacterial blooms: A player in the freshwater environmental resistome with public health relevance?, Environ. Res. 216 (2023) 114612. https://doi.org/10.1016/j.envres.2022.114612.

[6] J.C. Ho, A.M. Michalak, N. Pahlevan, Widespread global increase in intense lake phytoplankton blooms since the 1980s, Nature 574 (2019) 667–670. https://doi.org/10.1038/s41586-019-1648-7.

[7] S.-S. Lin, S.-L. Shen, A. Zhou, H.-M. Lyu, Assessment and management of lake eutrophication: A case study in Lake Erhai, China, Sci. Total Environ. 751 (2021) 141618. https://doi.org/10.1016/j.scitotenv.2020.141618.

[8] H.W. Paerl, J. Huisman, Blooms like it hot, Science 320 (2008) 57–58. https://doi.org/10.1126/science.1155398.

[9] J. Merder, T. Harris, G. Zhao, D.M. Stasinopoulos, R.A. Rigby, A.M. Michalak, Geographic redistribution of microcystin hotspots in response to climate warming, Nat. Water 1 (2023) 844–854. https://doi.org/10.1038/s44221-023-00138-w.

[10] B. Li, J. Qi, F. Liu, R. Zhao, M. Arabi, A. Ostovan, J. Song, X. Wang, Z. Zhang, L. Chen, Molecular imprinting-based indirect fluorescence detection strategy implemented on paper chip for non-fluorescent microcystin, Nat. Commun. 14 (2023) 6553. https://doi.org/10.1038/s41467-023-42244-z.

[11] Q. He, W. Wang, Q. Xu, Z. Liu, J. Teng, H. Yan, X. Liu, Microcystins in water: Detection, microbial degradation strategies, and mechanisms, Int. J. Environ. Res. Public Health 19 (2022) 13175. https://doi.org/10.3390/ijerph192013175.

[12] M.R. Teixeira, M.J. Rosa, Comparing dissolved air flotation and conventional sedimentation to remove cyanobacterial cells of *Microcystis aeruginosa*: Part I: The

key operating conditions, Sep. Purif. Technol. 52 (2006) 84–94. https://doi.org/10.1016/j.seppur.2006.03.017.

[13] H. Xu, Z. Tang, Z. Liang, H. Chen, X. Dai, Neglected methane production and toxicity risk in low-frequency ultrasound for controlling harmful algal blooms, Environ. Res. 232 (2023) 116422. https://doi.org/10.1016/j.envres.2023.116422.

[14] S. Sun, Q. Tang, H. Xu, Y. Gao, W. Zhang, L. Zhou, Y. Li, J. Wang, C. Song, A comprehensive review on the photocatalytic inactivation of *Microcystis aeruginosa*: Performance, development, and mechanisms, Chemosphere 312 (2023) 137239. https://doi.org/10.1016/j.chemosphere.2022.137239.

[15] F.A. Kibuye, A. Zamyadi, E.C. Wert, A critical review on operation and performance of source water control strategies for cyanobacterial blooms: Part I-chemical control methods, Harmful Algae 109 (2021) 102099. https://doi.org/10.1016/j.hal.2021.102099.

[16] L. He, Z. Lin, Y. Wang, X. He, J. Zhou, M. Guan, J. Zhou, Facilitating harmful algae removal in fresh water via joint effects of multi-species algicidal bacteria, J. Hazard. Mater. 403 (2021) 123662. https://doi.org/10.1016/j.jhazmat.2020.123662.

[17] L. Song, Y. Jia, B. Qin, R. Li, W.W. Carmichael, N. Gan, H. Xu, K. Shan, A. Sukenik, Harmful cyanobacterial blooms: Biological traits, mechanisms, risks, and control strategies, Annu. Rev. Environ. Resour. 48 (2023) 123–147. https://doi.org/10.1146/annurev-environ-112320-081653.

[18] M. Pal, P.J. Yesankar, A. Dwivedi, A. Qureshi, Biotic control of harmful algal blooms (HABs): A brief review, J. Environ. Manage. 268 (2020) 110687. https://doi.org/10.1016/j.jenvman.2020.110687.

583 [19] G. Zeng, R. Zhang, D. Liang, F. Wang, Y. Han, Y. Luo, P. Gao, Q. Wang, Q.
584 Wang, C. Yu, L. Jin, D. Sun, Comparison of the advantages and disadvantages of
585 algae removal technology and its development status, Water 15 (2023) 1104.
586 https://doi.org/10.3390/w15061104.
587 [20] J. Cui, X. Niu, D. Zhang, J. Ma, X. Zhu, X. Zheng, Z. Lin, M. Fu, The novel
588 chitosan-amphoteric starch dual flocculants for enhanced removal of *Microcystis*
589 *aeruginosa* and algal organic matter, Carbohydr. Polym. 304 (2023) 120474.
590 https://doi.org/10.1016/j.carbpol.2022.120474.
591 [21] R.S. Arruda, N.P. Noyma, L. de Magalhães, M.C.B. Mesquita, É.C. de Almeida, E.
592 Pinto, M. Lürling, M.M. Marinho, 'Floc and Sink' technique removes cyanobacteria
593 and microcystins from tropical reservoir water, Toxins 13 (2021) 405.
594 https://doi.org/10.3390/toxins13060405.
595 [22] D. de Lucena-Silva, J. Molozzi, J. dos S. Severiano, V. Becker, J.E. de Lucena
596 Barbosa, Removal efficiency of phosphorus, cyanobacteria and cyanotoxins by the
597 "flock & sink" mitigation technique in semi-arid eutrophic waters, Water Res. 159
598 (2019) 262–273. https://doi.org/10.1016/j.watres.2019.04.057.
599 [23] N.P. Noyma, L. de Magalhães, L.L. Furtado, M. Mucci, F. van Oosterhout, V.L.M.
600 Huszar, M.M. Marinho, M. Lürling, Controlling cyanobacterial blooms through
601 effective flocculation and sedimentation with combined use of flocculants and
602 phosphorus adsorbing natural soil and modified clay, Water Res. 97 (2016) 26–38.
603 https://doi.org/10.1016/j.watres.2015.11.057.

[24] F.P. Camacho, V.S. Sousa, R. Bergamasco, M. Ribau Teixeira, The use of *Moringa oleifera* as a natural coagulant in surface water treatment, Chem. Eng. J. 313 (2017) 226–237. https://doi.org/10.1016/j.cej.2016.12.031.

[25] Y. Yuan, H. Zhang, G. Pan, Flocculation of cyanobacterial cells using coal fly ash modified chitosan, Water Res. 97 (2016) 11–18. https://doi.org/10.1016/j.watres.2015.12.003.

[26] Z. Yu, X. Song, X. Cao, Y. Liu, Mitigation of harmful algal blooms using modified clays: Theory, mechanisms, and applications, Harmful Algae 69 (2017) 48–64. https://doi.org/10.1016/j.hal.2017.09.004.

[27] I. Gardi, Y.-G. Mishael, M. Lindahl, A.M. Muro-Pastor, T. Undabeytia, Coagulation-flocculation of *Microcystis aeruginosa* by polymer-clay based composites, J. Clean. Prod. 394 (2023) 136356. https://doi.org/10.1016/j.jclepro.2023.136356.

[28] J. Chen, G. Pan, Harmful algal blooms mitigation using clay/soil/sand modified with xanthan and calcium hydroxide, J. Appl. Phycol. 24 (2012) 1183–1189. https://doi.org/10.1007/s10811-011-9751-7.

[29] G. Pan, H. Zou, H. Chen, X. Yuan, Removal of harmful cyanobacterial blooms in Taihu Lake using local soils III. Factors affecting the removal efficiency and an *in situ* field experiment using chitosan-modified local soils, Environ. Pollut. 141 (2006) 206–212. https://doi.org/10.1016/j.envpol.2005.08.047.

[30] R. Sapra, R.P. Verma, G.P. Maurya, S. Dhawan, J. Babu, V. Haridas, Designer peptide and protein dendrimers: A cross-sectional analysis, Chem. Rev. 119 (2019) 11391–11441. https://doi.org/10.1021/acs.chemrev.9b00153.

[31] S. Mukherjee, S. Mukherjee, M.A.S. Abourehab, A. Sahebkar, P. Kesharwani, Exploring dendrimer-based drug delivery systems and their potential applications in cancer immunotherapy, Eur. Polym. J. 177 (2022) 111471. https://doi.org/10.1016/j.eurpolymj.2022.111471.

[32] Z. Lyu, L. Ding, A. Tintaru, L. Peng, Self-Assembling supramolecular dendrimers for Biomedical Applications: Lessons Learned from poly(amidoamine) dendrimers, Acc. Chem. Res. 53 (2020) 2936–2949. https://doi.org/10.1021/acs.accounts.0c00589.

[33] J. Chen, D. Zhu, X. Liu, L. Peng, Amphiphilic dendrimer vectors for RNA delivery: State-of-the-art and future perspective, Acc. Mater. Res. 3 (2022) 484–497. https://doi.org/10.1021/accountsmr.1c00272.

[34] X. Wang, M. Zhang, Y. Li, H. Cong, B. Yu, Y. Shen, Research status of dendrimer micelles in tumor therapy for drug delivery, Small 19 (2023) 2304006. https://doi.org/10.1002/smll.202304006.

[35] C. Galanakou, D. Dhumal, L. Peng, Amphiphilic dendrimers against antibiotic resistance: light at the end of the tunnel? Biomater. Sci. 11 (2023) 3379–3393. https://doi.org/10.1039/D2BM01878K.

[36] R. Rippka, J. Deruelles, J.B. Waterbury, M. Herdman, R.Y. Stanier, Generic assignments, strain histories and properties of pure cultures of cyanobacteria, Microbiology 111 (1979) 1–61. https://doi.org/10.1099/00221287-111-1-1.

[37] D. Zhu, H. Zhang, Y. Huang, B. Lian, C. Ma, L. Han, Y. Chen, S. Wu, N. Li, W. Zhang, X. Liu, A Self-assembling amphiphilic peptide dendrimer-based drug

649 delivery system for cancer therapy, Pharmaceutics 13 (2021) 1092.
650 https://doi.org/10.3390/pharmaceutics13071092.
651 [38] C. Ma, D. Zhu, Y. Chen, Y. Dong, W. Lin, N. Li, W. Zhang, X. Liu, Amphiphilic
652 peptide dendrimer-based nanovehicles for safe and effective siRNA delivery,
653 Biophys. Rep. 6 (2020) 278–289. https://doi.org/10.1007/s41048-020-00120-z.
654 [39] J. Graham, K. Loftin, A. C. Ziegler, M. Meyer, Guidelines for design and sampling
655 for cyanobacterial toxin and taste-and-odor studies in lakes and reservoirs. U.S.
656 Geological Survey Scientific Investigations Report 2008—5038, 2008.
657 https://doi.org/10.3133/SIR20085038
658 [40] P. Li, L. Zhang, W. Wang, J. Su, L. Feng, Rapid catalytic microwave method to
659 damage *Microcystis aeruginosa* with $FeCl_3$-loaded active carbon, Environ. Sci.
660 Technol. 45 (2011) 4521–4526. https://doi.org/10.1021/es200057g.
661 [41] J. Xiao, Y. Chen, M. Xue, R. Ding, Y. Kang, P.-L. Tremblay, T. Zhang, Fast-
662 growing cyanobacteria bio-embedded into bacterial cellulose for toxic metal
663 bioremediation, Carbohydr. Polym. 295 (2022) 119881.
664 https://doi.org/10.1016/j.carbpol.2022.119881.
665 [42] X. Zheng, X. Niu, D. Zhang, X. Ye, J. Ma, M. Lv, Z. Lin, Removal of *Microcystis*
666 *aeruginosa* by natural pyrite-activated persulfate: Performance and the significance
667 of iron species, Chem. Eng. J. 428 (2022) 132565.
668 https://doi.org/10.1016/j.cej.2021.132565.
669 [43] L.-M. Lei, Y.-S. Wu, N.-Q. Gan, L.-R. Song, An ELISA-like time-resolved
670 fluorescence immunoassay for microcystin detection, Clin. Chim. Acta 348 (2004)
671 177–180. https://doi.org/10.1016/j.cccn.2004.05.019.

[44] J. Yu, M. Liberton, P.F. Cliften, R.D. Head, J.M. Jacobs, R.D. Smith, D.W. Koppenaal, J.J. Brand, H.B. Pakrasi, *Synechococcus elongatus* UTEX 2973, a fast growing cyanobacterial chassis for biosynthesis using light and CO_2, Sci. Rep. 5 (2015) 8132. https://doi.org/10.1038/srep08132.

[45] K. Schulze, D.A. López, U.M. Tillich, M. Frohme, A simple viability analysis for unicellular cyanobacteria using a new autofluorescence assay, automated microscopy, and ImageJ, BMC Biotechnol. 11 (2011) 118. https://doi.org/10.1186/1472-6750-11-118.

[46] E. Beck, R. Scheibe, Senescence and ageing in plants and cyanobacteria, Physiol. Plant. 119 (2003) 1–4. https://doi.org/10.1034/j.1399-3054.2003.00140.x.

[47] H. Pei, H. Xu, H. Xiao, J. Sun, W. Hu, X. Li, C. Ma, Y. Jin, Using a novel hydrogen-terminated porous Si wafer to enhance *Microcystis aeruginosa* effective removal by chitosan at a low dosage, Colloids Surf. A Physicochem. Eng. Asp. 499 (2016) 88–96. https://doi.org/10.1016/j.colsurfa.2016.04.015.

[48] D. Dhumal, B. Maron, E. Malach, Z. Lyu, L. Ding, D. Marson, E. Laurini, A. Tintaru, B. Ralahy, S. Giorgio, S. Pricl, Z. Hayouka, L. Peng, Dynamic self-assembling supramolecular dendrimer nanosystems as potent antibacterial candidates against drug-resistant bacteria and biofilms, Nanoscale 14 (2022) 9286–9296. https://doi.org/10.1039/D2NR02305A.

[49] C.C. Lee, J.A. MacKay, J.M.J. Fréchet, F.C. Szoka, Designing dendrimers for biological applications, Nat. Biotechnol. 23 (2005) 1517–1526. https://doi.org/10.1038/nbt1171.

694 [50] Y. Dong, Y. Chen, D. Zhu, K. Shi, C. Ma, W. Zhang, P. Rocchi, L. Jiang, X. Liu,
695 Self-assembly of amphiphilic phospholipid peptide dendrimer-based nanovectors
696 for effective delivery of siRNA therapeutics in prostate cancer therapy, J. Control.
697 Release 322 (2020) 416–425. https://doi.org/10.1016/j.jconrel.2020.04.003.
698 [51] X. Zhang, X. Xu, Y. Li, C. Hu, Z. Zhang, Z. Gu, Virion-like membrane-breaking
699 nanoparticles with tumor-activated cell-and-tissue dual-penetration conquer
700 impermeable cancer, Adv. Mater. 30 (2018) 1707240.
701 https://doi.org/10.1002/adma.201707240.
702 [52] Y. Guo, H. Meng, S. Zhao, Z. Wang, L. Zhu, D. Deng, J. Liu, H. He, W. Xie, G.
703 Wang, L. Zhang, How does *Microcystis aeruginosa* respond to elevated
704 temperature?, Sci. Total Environ. 889 (2023) 164277.
705 https://doi.org/10.1016/j.scitotenv.2023.164277.
706 [53] J. Zhu, Z. Yu, L. He, Y. Jiang, X. Cao, X. Song, The molecular mechanisms and
707 environmental effects of modified clay control algal blooms in aquacultural water, J.
708 Environ. Manage. 337 (2023) 117715.
709 https://doi.org/10.1016/j.jenvman.2023.117715.
710 [54] A. Sukenik, Y. Viner-Mozzini, M. Tavassi, S. Nir, Removal of cyanobacteria and
711 cyanotoxins from lake water by composites of bentonite with micelles of the cation
712 octadecyltrimethyl ammonium (ODTMA), Water Res. 120 (2017) 165–173.
713 https://doi.org/10.1016/j.watres.2017.04.075.
714 [55] G. Pan, M.-M. Zhang, H. Chen, H. Zou, H. Yan, Removal of cyanobacterial blooms
715 in Taihu Lake using local soils. I. Equilibrium and kinetic screening on the
716 flocculation of *Microcystis aeruginosa* using commercially available clays and

minerals, Environ. Pollut. 141 (2006) 195–200. https://doi.org/10.1016/j.envpol.2005.08.041.

[56] M. Suárez, E. García-Romero, Variability of the surface properties of sepiolite, Appl. Clay Sci. 67–68 (2012) 72–82. https://doi.org/10.1016/j.clay.2012.06.003.

[57] M.Y. Han, W. Kim, A theoretical consideration of algae removal with clays, Microchem. J. 68 (2001) 157–161. https://doi.org/10.1016/S0026-265X(00)00142-9.

[58] S. Zhang, X. Du, H. Liu, M.D. Losiewic, X. Chen, Y. Ma, R. Wang, Z. Tian, L. Shi, H. Guo, H. Zhang, The latest advances in the reproductive toxicity of microcystin-LR, Environ. Res. 192 (2021) 110254. https://doi.org/10.1016/j.envres.2020.110254.

[59] J. Li, L. Cao, Y. Yuan, R. Wang, Y. Wen, J. Man, Comparative study for microcystin-LR sorption onto biochars produced from various plant- and animal-wastes at different pyrolysis temperatures: Influencing mechanisms of biochar properties, Bioresour. Technol. 247 (2018) 794–803. https://doi.org/10.1016/j.biortech.2017.09.120.

[60] C. Zhou, H. Chen, H. Zhao, Q. Wang, Microcystin biosynthesis and toxic effects, Algal Res. 55 (2021) 102277. https://doi.org/10.1016/j.algal.2021.102277.

[61] L. Peng, L. Lei, L. Xiao, B. Han, Cyanobacterial removal by a red soil-based flocculant and its effect on zooplankton: an experiment with deep enclosures in a tropical reservoir in China, Environ. Sci. Pollut. Res. 26 (2019) 30663–30674. https://doi.org/10.1007/s11356-018-2572-3.

[62] J. Liu, C. Chen, T. Wei, O. Gayet, C. Loncle, L. Borge, N. Dusetti, X. Ma, D. Marson, E. Laurini, S. Pricl, Z. Gu, J. Iovanna, L. Peng, X.-J. Liang, Dendrimeric nanosystem consistently circumvents heterogeneous drug response and resistance in pancreatic cancer, Exploration 1 (2021) 21–34. https://doi.org/10.1002/EXP.20210003.

[63] S. Wei, G. Zhuang, L. Cheng, S. Wang, The proliferation rule of *Microcystis aeruginosa* under different initial pH conditions and its influence on the pH value of the environment, Environ. Sci. Pollut. Res. 29 (2022) 13835–13844. https://doi.org/10.1007/s11356-021-16719-9.

[64] C.A. Amorim, A. do N. Moura, Ecological impacts of freshwater algal blooms on water quality, plankton biodiversity, structure, and ecosystem functioning, Sci. Total Environ. 758 (2021) 143605. https://doi.org/10.1016/j.scitotenv.2020.143605.

[65] L.E. Krausfeldt, A.T. Farmer, H.F. Castro Gonzalez, B.N. Zepernick, S.R. Campagna, S.W. Wilhelm, Urea is both a carbon and nitrogen source for *Microcystis aeruginosa*: Tracking 13C incorporation at bloom pH conditions, Front. Microbiol. 10 (2019) 1064. https://doi.org/10.3389/fmicb.2019.01064

Figure legends

Scheme 1. Amphiphilic peptide dendrimers (AmPDs) and their use in the flocculation of *M. aeruginosa*. Both the AmPDs, KK_2 and KK_2K_4, form positively charged nanoassemblies that will interact with the negatively charged surface of *M. aeruginosa* cells, leading to microbial aggregation and the formation of dense flocs that will sink and can be removed from the treated aqueous solution. In the presence of sepiolite clay, AmPD-driven flocculation becomes more efficient. The AmPD nanoassemblies coat sepiolite spindles, which quickly form flocs with cyanobacteria.

Fig. 1. The removal of *M. aeruginosa* by AmPD nanoassemblies. (a) Removal of cyanobacteria and (b) remaining turbidity after 30 min of flocculation treatment with different concentrations of KK_2 or KK_2K_4. (c) Time-course curves of cyanobacterial cell removal with 6.0 mg/L KK_2 or 5.0 mg/L KK_2K_4. (d) Digital images of untreated *M. aeruginosa or* cultures treated with either KK_2 or KK_2K_4. FTU: Formazin Turbidity Unit.

Fig. 2. Light microscopy, SEM, and zeta potential analyses of *M. aeruginosa* aggregates with the AmPDs KK_2 and KK_2K_4. Light micrographs of (a) untreated *M. aeruginosa* and *M. aeruginosa* treated with (b) 2.0, (c) 4.0, and (d) 6.0 mg/L KK_2 or (e) 1.0, (f) 3.0, and (g) 5.0 mg/L KK_2K_4. SEM micrographs of (h) untreated *M. aeruginosa* and *M. aeruginosa* treated with (i) 6.0 mg/L KK_2 or (j) 5.0 mg/L KK_2K_4 nanoassemblies. (k) Zeta potentials of cyanobacteria, AmPDs, and cyanobacteria with either one of the AmPDs presented in a bar graph. MA: *M. aeruginosa*.

Fig. 3. The flocculation of *M. aeruginosa* by AmPD nanoassemblies combined with sepiolite. (a) Removal of cyanobacteria after 15 min of treatment with 200.0 mg/L sepiolite and different concentrations of KK_2 or KK_2K_4. (b) Time-course curves of cyanobacterial cell removal with 200.0 mg/L sepiolite and either 4.0 mg/L KK_2 or 3.0 mg/L KK_2K_4. (c) Removal of cyanobacteria with either 4.0 mg/L KK_2 or 3.0 mg/L KK_2K_4 nanoassemblies and different concentrations of sepiolite clay from 0 to 325.0 mg/L. (d-g) Digital images of untreated *M. aeruginosa or* cultures treated with sepiolite alone, and sepiolite with either KK_2 or KK_2K_4. FTU: Formazin Turbidity Unit.

Fig. 4. Light microscopy, SEM, and zeta potential analyses of *M. aeruginosa* aggregates with AmPDs and sepiolite. Light micrographs of the cyanobacteria treated with (a) 4.0 mg/L KK_2 only or KK_2 with (b) 50.0, (c) 100.0, and (d) 200.0 mg/L sepiolite. Micrographs of *M. aeruginosa* treated with (e) 3.0 mg/L KK_2K_4 only or KK_2K_4 with (f) 50.0, (g) 100.0, and (h) 200.0 mg/L sepiolite. Red arrows indicate sepiolite particles. SEM micrographs of (i) untreated *M. aeruginosa* and *M. aeruginosa* treated with a combination of (j) KK_2 and sepiolite or (k) KK_2K_4 and sepiolite. (l) Zeta potential bar graph of sepiolite, AmPDs with sepiolite, and cyanobacteria with sepiolite in combination with either one of the AmPDs. MA: *M. aeruginosa*, Sep.: sepiolite.

Fig. 5. The impact of AmPDs and sepiolite on *M. aeruginosa* viability, extracellular MC-LR concentration, and floc stability. (a) *M. aeruginosa* viability 0.5 h and 24 h after different treatments. (b) Extracellular MC-LR concentrations at the end of the flocculation processes with AmPDs and sepiolite. (c) Filtration evaluation of the integrity of the different types of floc. Sep.: sepiolite.

Fig. 6. Effect of salinity and pH on the AmPD-driven flocculation processes. The flocculation of *M aeruginosa* by KK_2 or KK_2K_4 nanoassemblies at different salinity (a) without and (b) with sepiolite, and at different pH (c) without and (d) with sepiolite. FTU: Formazin Turbidity Unit.

Revised Scheme 1

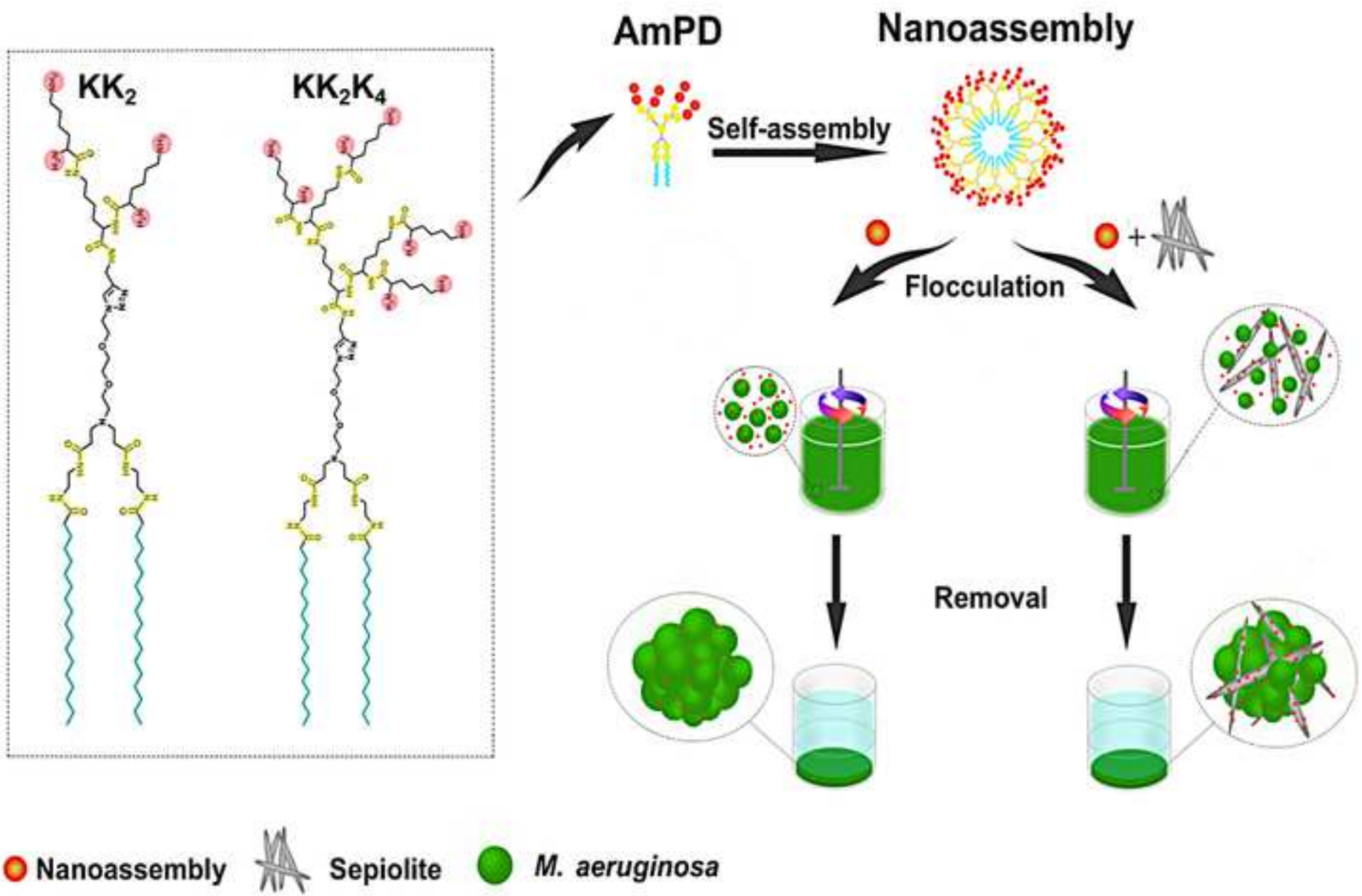

Pasted Layer

Revised Figure 1

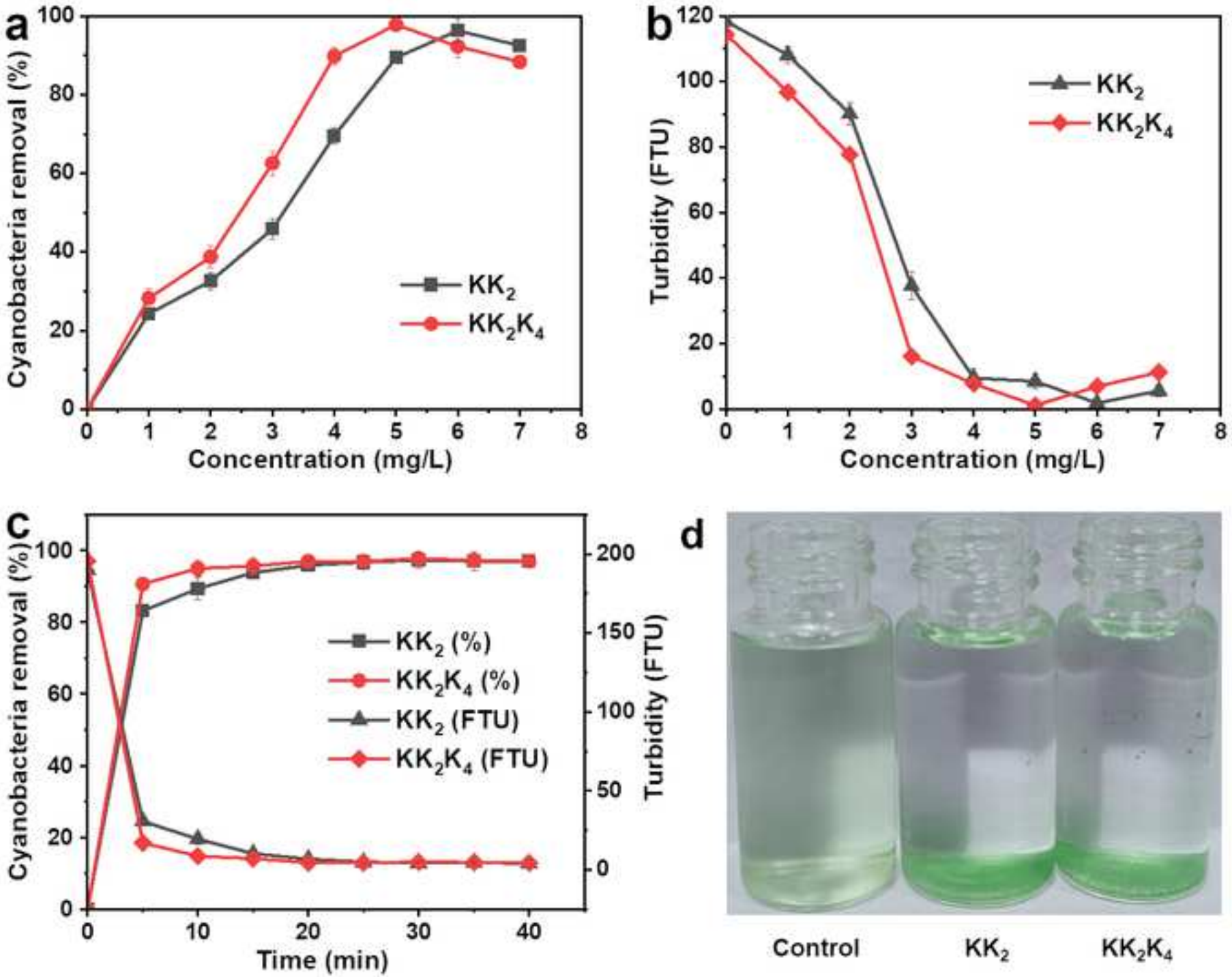

Pasted Layer

Revised Figure 2

Pasted Layer

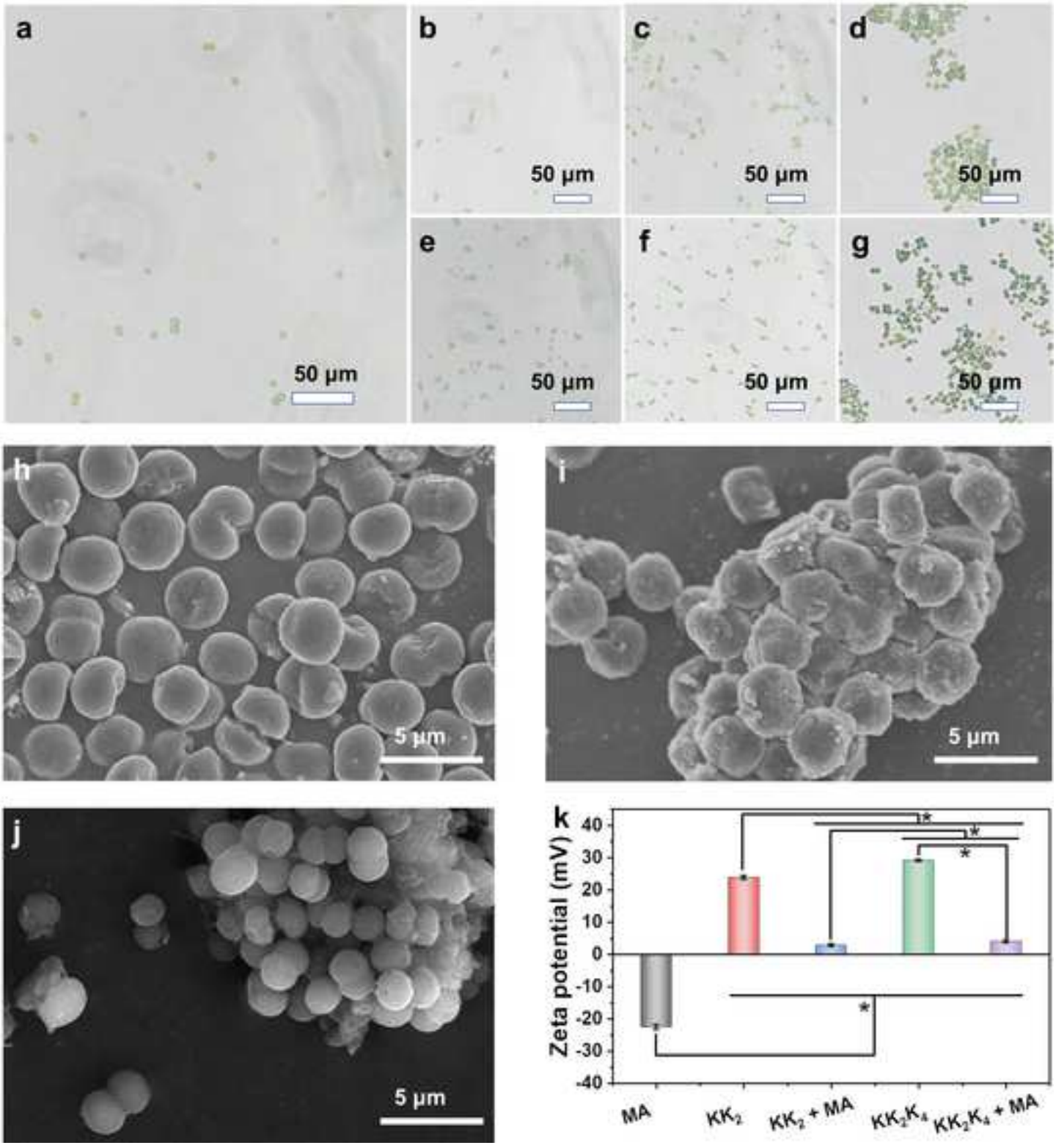

Revised Figure 3

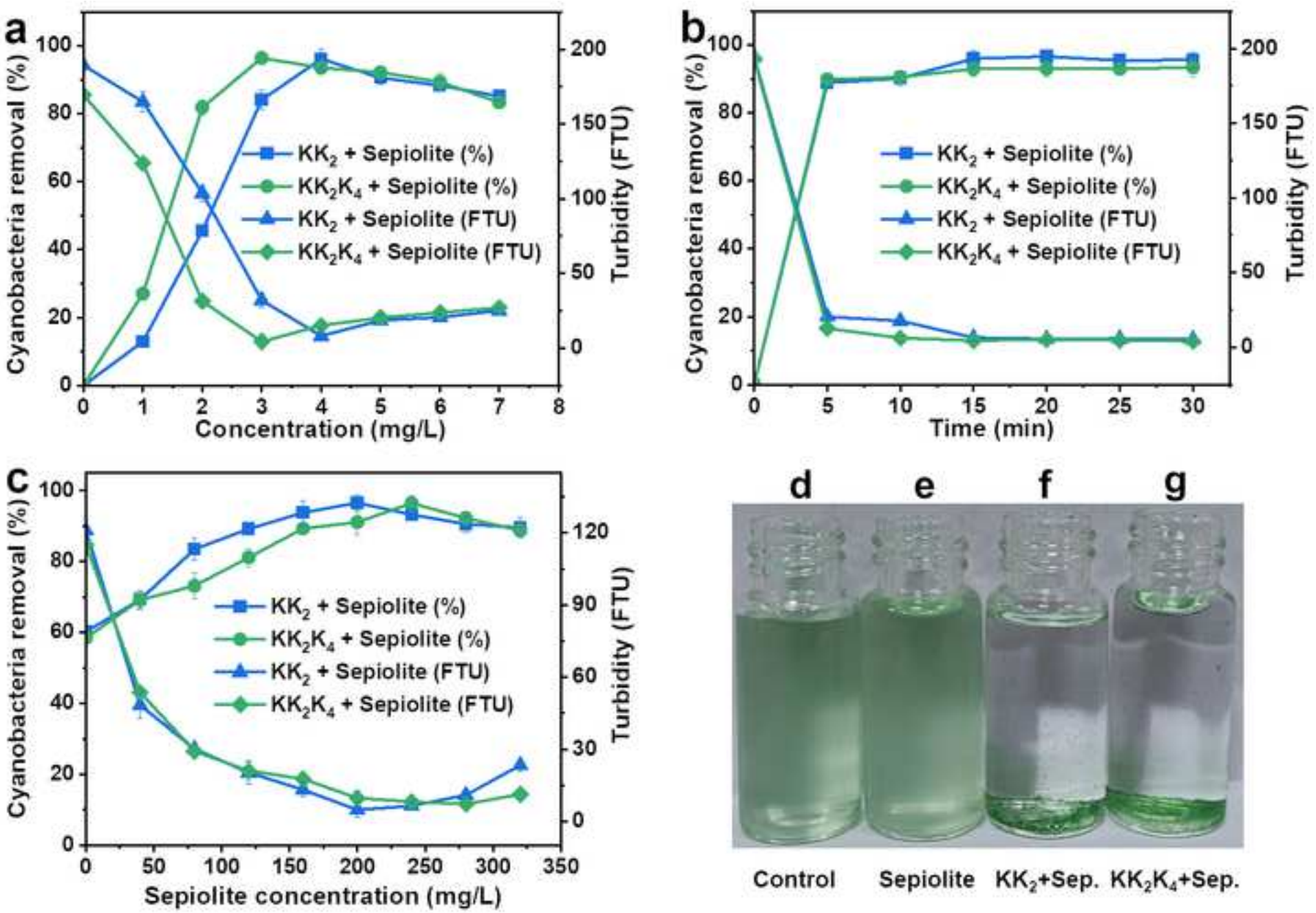

Pasted Layer

Revised Figure 4

Pasted Layer

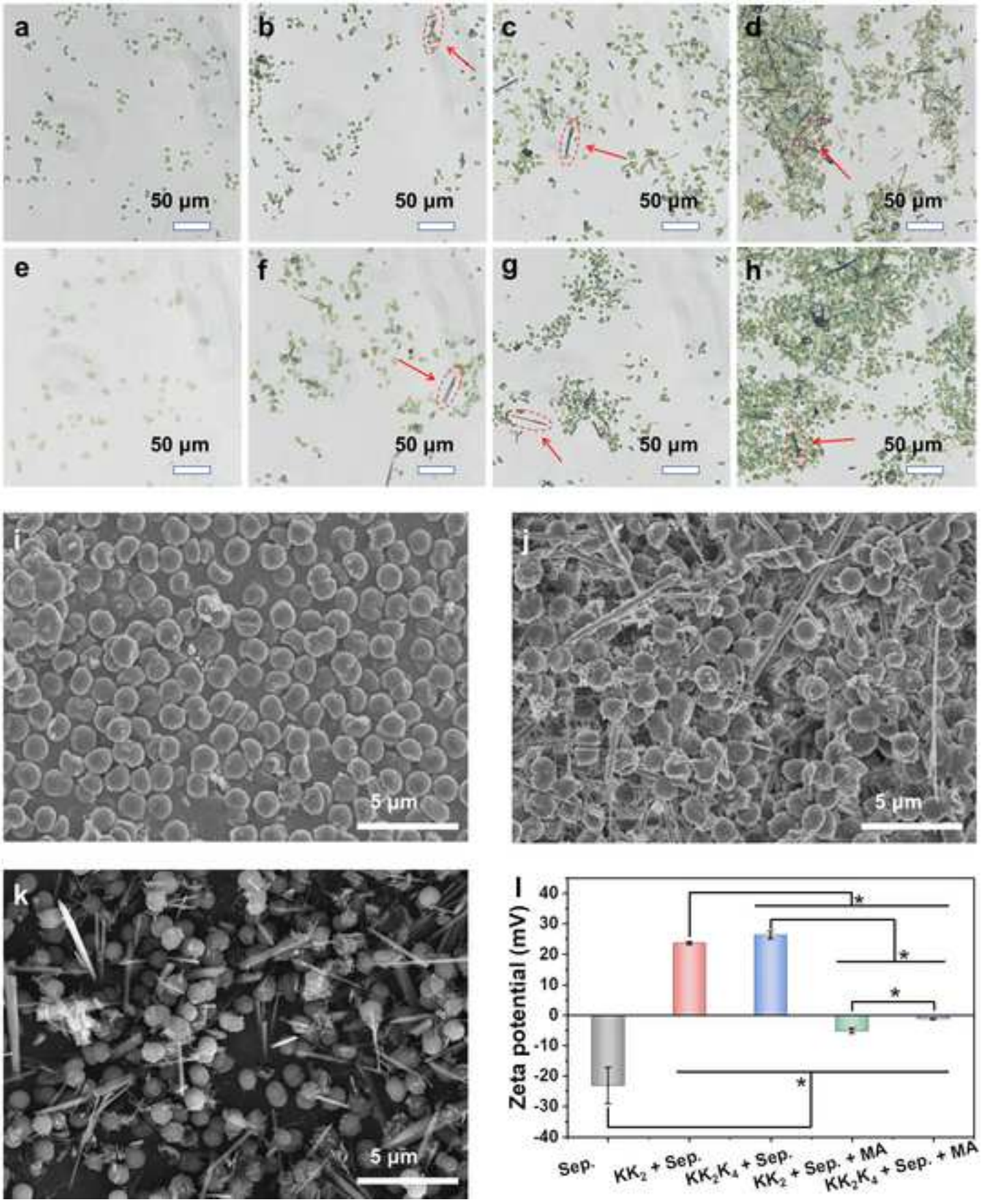

Revised Figure 5

Pasted Layer

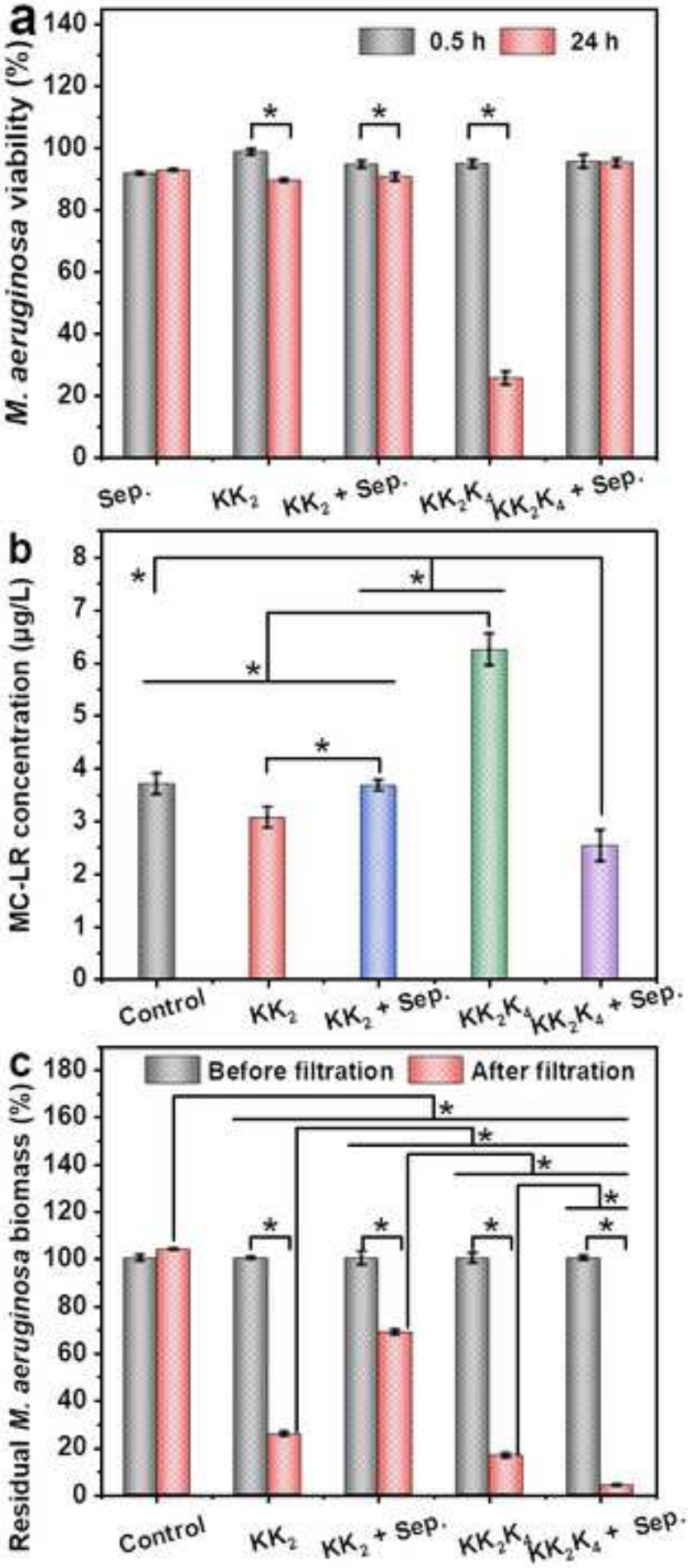

Revised Figure 6

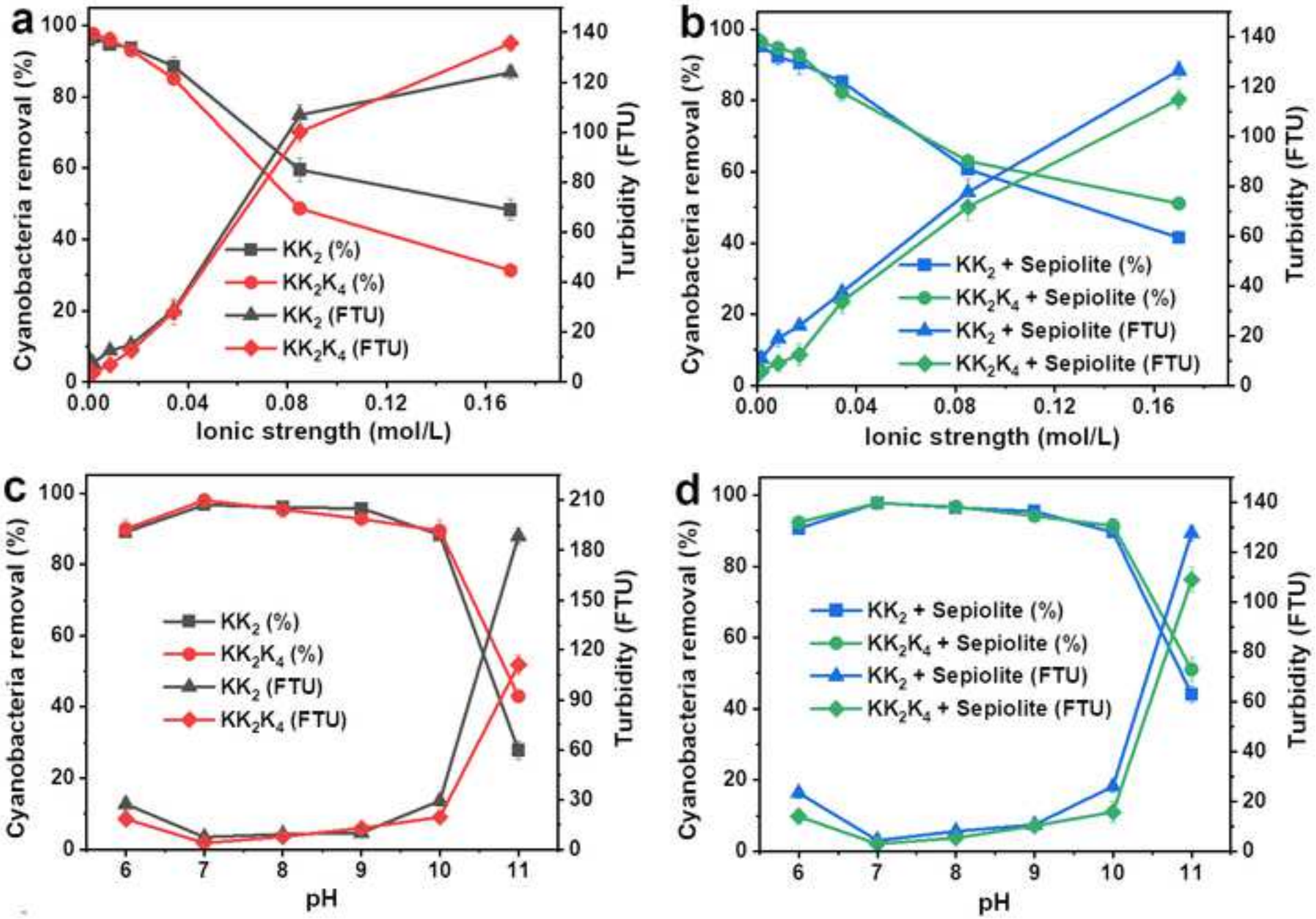

Pasted Layer